Since January 2020 Elsevier has created a COVID-19 resource centre with free information in English and Mandarin on the novel coronavirus COVID-19. The COVID-19 resource centre is hosted on Elsevier Connect, the company's public news and information website.

Journal of Hazardous Materials 423 (2022) 127152

Contents lists available at ScienceDirect

Journal of Hazardous Materials

journal homepage: www.elsevier.com/locate/jhazmat

Research Paper

Residual chlorine disrupts the microbial communities and spreads antibiotic resistance in freshwater

Zhenyan Zhang [a,1], Qi Zhang [a,1], Tao Lu [a], Jieyu Zhang [a], Liwei Sun [a], Baolan Hu [b], Jun Hu [a], Josep Peñuelas [c,d], Lizhong Zhu [b,e,*], Haifeng Qian [a,**]

[a] College of Environment, Zhejiang University of Technology, Hangzhou, Zhejiang 310032, PR China
[b] Department of Environmental Science, Zhejiang University, Hangzhou, Zhejiang 310058, PR China
[c] CSIC, Global Ecology Unit CREAF-CSIC-UAB, Bellaterra, 08193 Barcelona, Catalonia, Spain
[d] CREAF, Cerdanyola del Vallès, 08193 Barcelona, Catalonia, Spain
[e] Zhejiang Provincial Key Laboratory of Organic Pollution Process and Control, Hangzhou, Zhejiang 310058, PR China

ARTICLE INFO

Editor: Dr. G. Jianhua

Keywords:
Residual chlorine
Aquatic toxicity
Microbial community
Ecotoxicity
Antibiotic-resistance genes

ABSTRACT

Chlorine disinfection is a key global public health strategy for the prevention and control of diseases, such as COVID-19. However, little is known about effects of low levels of residual chlorine on freshwater microbial communities and antibiotic resistomes. Here, we treated freshwater microcosms with continuous low concentrations of chlorine and quantified the effects on aquatic and zebrafish intestinal microbial communities and antibiotic resistomes, using shotgun metagenome and 16S rRNA gene sequencing. Although chlorine rapidly degraded, it altered the aquatic microbial community composition over time and disrupted interactions among microbes, leading to decreases in community complexity and stability. However, community diversity was unaffected. The majority of ecological functions, particularly metabolic capacities, recovered after treatment with chlorine for 14 d, due to microbial community redundancy. There were also increased levels of antibiotic-resistance gene dissemination by horizontal and vertical gene transfer under chlorine treatment. Although the zebrafish intestinal microbial community recovered from temporary dysbiosis, growth and behavior of zebrafish adults were negatively affected by chlorine. Overall, our findings demonstrate the negative effects of residual chlorine on freshwater ecosystems and highlight a possible long-term risk to public health.

1. Introduction

Following its outbreak at the end of 2019, COVID-19 spread rapidly and was declared a global pandemic on 11 March 2020 (World Health Organization, 2020a). Chlorine-containing disinfectants act as oxidizing biocides and recommendations were made for their use in the decontamination of surfaces for COVID-19 infection control (Wang et al., 2020b). According to advice provided by the WHO (World Health Organization, 2020b), residual chlorine in drinking water distribution systems must be maintained at > 0.5 mg/L for effective control of COVID-19, while research indicated that effective concentrations of residual chlorine for treatment of wastewater should be > 6.5 mg/L (Wang et al., 2020a). However, this extensive use of chlorine-containing disinfectants leads to releases of residual chlorine and other byproducts into the environment, particularly to freshwater habitats (Lu and Guo, 2021). It has been reported that during February and March of 2020, the beginning of COVID-19 epidemic, concentrations of residual chlorine in some lakes of China remained mostly undetectable, however, it increased up to 0.4 mg/L in parts of lakes in Wuhan (Chu et al., 2021), the central city of epidemic with the heavy usage of chlorine-containing disinfectants. Despite its rapid degradation, there is an urgent need to quantify and assess the environmental impacts of these continual and low dose discharges of chlorine to natural aquatic systems.

Residual chlorine derived from chlorine-containing disinfectants, which comprise hypochlorite ions, hypochlorous acid, and chloride, elicits a range of toxicological effects on nontarget organisms, such as zebrafish (Ding et al., 2020), planaria (Rodrigues Macêdo et al., 2019), dinoflagellates (Ebenezer and Ki, 2014), and green algae (Vannoni et al.,

* Corresponding author at: Department of Environmental Science, Zhejiang University, Hangzhou, Zhejiang 310058, PR China.
** Corresponding author.
E-mail addresses: zlz@zju.edu.cn (L. Zhu), hfqian@zjut.edu.cn (H. Qian).
[1] Zhenyan Zhang and Qi Zhang contributed equally to this work.

https://doi.org/10.1016/j.jhazmat.2021.127152
Received 4 June 2021; Received in revised form 5 August 2021; Accepted 3 September 2021
Available online 9 September 2021

2018). The development of omics biotechnology has enabled research to focus on pollutant ecotoxicity to microbes at the more complex community level than the simple single organism level, that allows for more comprehensive ecotoxicity assessment of anthropogenic disturbance (Lu et al., 2019; Ma et al., 2019). Continuous chlorine disinfection has been found to disrupt normal shifts in bacteria community composition that occur in full-scale cooling water systems, by triggering the growth of particular bacteria species (Pinel et al., 2020). Low concentrations (approx. 0.25 mg/L) of residual chlorine dioxide disinfectants in irrigation water were shown to directly affect bacterial communities in water, but not those in soil or spinach crops (Truchado et al., 2018). Changes in microbial community structure and function potential were recorded in drinking water distribution systems due to selective pressures driven by chlorine disinfection (Dai et al., 2020). Besides, Lu et al. Lu and Guo (2021) expounded the spreads of antimicrobial resistance were accelerated by the increasing use of disinfectants in COVID-19. However, there are environmental health uncertainties associated with residual chlorine due to contrasting directional effects on the dissemination of antibiotic resistance genes (ARGs) (Jia et al., 2020; Li and Gu, 2019; Mantilla-Calderon et al., 2019). Given the negative effects of ARGs on human health when they are incorporated into living pathogenic bacteria (Chen et al., 2019), there is an urgent need to evaluate the impacts of residual chlorine on the transfer of ARGs in freshwater habitats.

A model was developed using unpolluted freshwater collected from a pond and Zebrafish to study the effect of continuous chlorine treatment on the structure and function of both the aquatic and fish intestinal microbiomes using 16S rRNA gene sequencing and metagenomics. We also quantified the abundance and transfer of ARGs during the study. This systematic study aimed to confirm the environmental risks of residual chlorine to freshwater microbial communities, including impacts on ARG transfer. Finally, we try to provide a theoretical basis for the rational application of chlorine-containing disinfectants to minimize environmental risks during disease control.

2. Materials and methods

2.1. Establishment of freshwater microcosms

Samples of water were collected from a depth of 0.5 m from an unpolluted pond, where active chlorine content was undetectable, at Zhejiang University of Technology, Hangzhou, China (30° 17′45.11″ N, 120° 09′ 50.07″ E), transported immediately to the laboratory. Water samples were placed under cool-white fluorescent light (46 μmol photons/(m^2 s)) with a 12-h light:12-h dark photoperiod at 25 ± 0.5 °C for 3 d to allow for adaptation and settling. As determined by a multiparameter water quality detector (Lohand Biological, Zhejiang, China), active chlorine was undetected in these water samples. Six-month-old adult zebrafish (*Danio rerio*) were purchased from the China Zebrafish Resource Center (Hubei, China) and allowed to adapt for 7 d under the same conditions as the water samples. After adaptation, we created nine microcosms each contained 2 L of pond water in a glass beaker, plus three healthy adult zebrafish.

Sodium hypochlorite (Blue Moon, Guangzhou, China) used in this study was purchased from a local supermarket during the outbreak of COVID-19 and contained 8–10.5 g/L active chlorine as described in the product label. During 14 d treatment, we measured the actual active chlorine of the sodium hypochlorite in Blue Moon every day and added sodium hypochlorite once a day to microcosms at the final concentrations of 0 (control), 0.01 and 0.1 mg/L of active chlorine. The actual active chlorine in the sodium hypochlorite was 8.05 g/L as we measured at the first day and there was no significant degradation of active chlorine in the Blue Moon during 14 d treatment. Each group had three biological replicates. For well dissolution of sodium hypochlorite in microcosm and reducing the impacts of dissolution on zebrafish as far as possible, about two-thirds of water in microcosm, without zebrafish, were pour into a new glass beaker and added sodium hypochlorite. After dissolved by a glass rod, this water was poured back to the microcosm sightly. The microcosms were sightly shook for further dissolution. The experimental concentrations of active chlorine were similar to those of residual chlorine recorded from in some rivers in China during the COVID-19 epidemic (up to 0.4 mg/L) (Chu et al., 2021). The microcosms were cultured under the adaptation conditions described above.

2.2. Determination of rate of active chlorine degradation

The levels of active chlorine content in microcosms were measured daily, using a multiparameter water quality detector (Lohand Biological, Zhejiang, China). However, the concentration of active chlorine in microcosms is too low to be detected after one day treatment. So, we carried out another experiment to determine the rate of active chlorine degradation in freshwater. We added sodium hypochlorite disinfectant at initial concentrations of 1.0, 2.0. 3.75, and 5.0 mg/L of active chlorine to three replicate samples of the pond water to ensure adequate levels of detection. And we continuously measured the levels of active chlorine content until it completely degraded (Fig. S1).

2.3. Measurement of microcosm physicochemical properties

Microcosm pH was measured using a pH meter (FE20, Mettler Toledo, Switzerland). Three samples of the microbiome were collected every 2 d from 50 mL of water filtered through a 0.45-μm membrane. Levels of total dissolved nitrogen (TDN) and total dissolved phosphorus (TDP) in the filtered water were measured using the methods described in a previous study (Zhang et al., 2021).

2.4. Microcosm metagenome sample preparation and sequencing

About 200 mL of water in each microcosm was filtered through 0.45-μm polycarbonate filters, as one sample, to collect aquatic microorganisms at 0, 7 and 14 d after treatment. Each treatment (control, 0.01 mg/L and 0.1 mg/L) had three biological replicates for metagenome. At the 0 day, we collected the samples immediately after establishment of freshwater microcosms. Therefore, microbial communities were similar in each microcosm, and only one replicated sample from each treatment was randomly chosen as 0 d samples for metagenome analysis. Samples were stored at − 80 °C immediately after collection. Total genomic DNA was extracted directly from the filter membranes using a DNA extraction kit (ALFA-SEQ Advanced Water DNA Kit, Guangdong Magigene Biotechnology Co., Ltd., Guangzhou, China) according to the manufacturer's instructions, and DNA concentration and purity were measured using a fluorometer (Qubit 2.0, Thermo Fisher Scientific, Waltham, USA) and spectrophotometer (NanoDrop One, Thermo Fisher Scientific, Waltham, USA) after DNA integrity and purity had been checked on 1% agarose gels. Sequence libraries were generated using a DNA library preparation kit (NEB Next Ultra DNA Library Prep Kit, New England Biolabs, MA, USA) following the manufacturer's instructions. The library quality was assessed by electrophoresis (Agilent 4200, Agilent, Santa Clara, CA) using a fluorometer (Qubit 3.0 Fluorometer, Life Technologies, Grand Island, NY). And sequencing was performed on an Illumina Novaseq platform (Illumina, CA, USA) at Guangdong Magigene Biotechnology Co., Ltd. (Guangzhou, China). Absolute abundance of bacteria was determined using real time qPCR analysis of total genomic DNA, as described by Zhang et al. (2020), based on the reasonable assumptions that the capture efficiency and extraction efficiency were equal between samples, because we used the same methods and materials for all samples.

2.5. Microcosm metagenome assembly and analysis

For each metagenome dataset, raw reads were filtered to remove those containing low-quality bases using Trimmomatic v0.36 (Bolger

et al., 2014) and to acquire clean data for subsequent analysis. MEGAHIT v1.0.6 (Li et al., 2015) was used for the de novo assembly of the clean data and to interrupt the assembled scaffold at N positions to leave scaftigs with unknown N bases. The reads that were not used in this step of all samples were combined and assembled in MEGAHIT. Open reading frames (ORFs) were predicted for each assembled scaftig (>500 bp) using MetaGeneMark v3.38 (Zhu et al., 2010), with default parameters. CD-HIT v4.7 (Fu et al., 2012) was used to remove redundant ORFs and obtain unique initial gene (unigene) clusters (95% identity with 90% coverage). Clean data for each sample were mapped to unigenes using BBMap (http://jgi.doe.gov/data-and-tools/bbtools/) to obtain the number of mapped reads, and calculation of gene abundance per sample, based on the number of mapped reads and length of the gene. We used a BLAST search of unigenes against the nonredundant (NR) database of NCBI and Kyoto Encyclopedia of Genes and Genomes (KEGG) (http://www.kegg.jp/kegg/) databases for taxonomic and functional annotations, respectively, using DIAMOND software v0.8.17.79 (https://github.com/bbuchfink/diamond/). NR results of which the e-value ≤ 1e-10 were chosen to take the LCA algorithm for system classification in MEGAN v6 (Huson et al., 2007), to ensure the correction of species annotation information of unigenes. Abundance information at each taxonomic level (kingdom, phylum, class, order, family, genus, species) was obtained based on the taxonomic classification and the abundance of unigenes. For KEGG results, the best BLAST hit (lowest e-value) was used for subsequent analysis. Relative abundance at each functional hierarchy (from KEGG Orthology (KO) to KEGG level 1) was equal to the sum of the relative abundance of unigenes annotated to that functional level. Unigenes were also BLAST searched against the Comprehensive Antibiotic Resistance Database (CARD) using DIAMOND software v0.8.17.79 (https://github.com/bbuchfink/diamond/) to identify the ARGs. Opportunistic human pathogens were detected by comparison between species table and an online database (https://www.bode-science-center.com/center/relevant-pathogens-from-a-z.html). The taxonomic annotation of each ARGs-carrying unigene were determined by comparison between species table and the ARG table. To reveal the HGT potential of ARGs, ARG-carrying contigs were also determined by BLAST searching against CARD, and then plasmid sequences for all ARG-carrying contigs were predicted using PlasFlow (Krawczyk et al., 2018). Abundance of chromosome-carried and plasmid-carried ARGs was calculated, respectively, as the sum of the abundance of contigs annotated to this ARG. The more details of microcosm metagenome assembly and analysis were provided in the Supplementary methods and Table S1.

2.6. Zebrafish intestinal microbe gene sampling and sequencing

At 0, 7, and 14 d after treatment, the entire intestines of one single zebrafish from each microcosm were aseptically dissected and collected. Samples from each group were separated into four subsamples and immediately frozen on dry ice and stored at − 80 °C prior to analysis. Each group had four biological replicates for 16S rRNA gene sequencing. Genomic DNA was extracted from the frozen samples using a DNA extraction kit (ALFA-SEQ Advanced Stool DNA Kit, Guangdong Magigene Biotechnology Co., Ltd., Guangzhou, China), following the manufacturer's instructions, and DNA concentration and purity were measured using a spectrophotometer (NanoDrop One, Thermo Fisher Scientific, MA, USA). We used the primers 338 F (5′-ACTCCTACGGGAGGCAGCAG-3′) and 806 R (5′-GGACTACHVGGGTWTCTAAT-3′) to amplify the V3-V4 region of the 16 S rRNA gene via thermocycler PCR (Bio-Rad Laboratory, CA, USA). The purified amplicons were sequenced (Illumina Nova6000, Illumina, CA, USA) at Guangdong Magigene Biotechnology Co., Ltd. (Guangzhou, China).

2.7. Intestinal sample 16S rRNA gene sequencing analysis

After quality of the raw data was confirmed by Fastp v0.14.1 (https://github.com/OpenGene/fastp), the primers were removed by using Cutadapt v2.10 (https://github.com/marcelm/cutadapt/). Paired-end clean reads were merged by using Usearch v10 (http://www.drive5.com/usearch/). Operational taxonomic unit (OTU) clustering was performed using Uparse v7.0.1090 (https://www.drive5.com/uparse/). Chimera sequences and singleton OTUs were simultaneously removed during clustering. Taxonomic annotation of each OTU was performed using the SILVA Database (https://www.arb-silva.de/) by Usearch v10 (http://www.drive5.com/usearch/) with the confidence threshold ≥ 0.8. OTUs and their tags that were annotated as chloroplasts or mitochondria and could not be annotated at the kingdom level were removed. OTU taxonomic information tables were generated and subsampled for relative abundance calculation and subsequent analysis. The more details of 16S rRNA gene sequencing analysis were provided in the Supplementary methods and Table S2.

2.8. Liver transcriptome analysis of zebrafish

The liver of one single zebrafish from each microcosm was aseptically dissected at 7 d of the experiment, immediately frozen on dry ice, and stored at − 80 °C prior to analysis. Each group had three biological replicates for transcriptome then. Total RNA was extracted using an RNA extraction kit (HiPure Universal RNA Midi Kit, Magen, Guangzhou, China), according to the manufacturer's instructions, while RNA quantity was determined using a fluorometer (Qubit 2.0, Thermo Fisher Scientific, MA, USA) and spectrophotometer (NanoDrop One, Thermo Fisher Scientific, MA, USA) simultaneously and RNA integrity was detected using electrophoresis (Agilent 2100, Agilent Technologies, Waldbron, Germany). Whole mRNAseq libraries were generated using an RNA library preparation kit (Next Ultra Nondirectional RNA Library Prep Kit for Illumina, New England Biolabs, MA, USA), following the manufacturer's instructions. Transcriptomes were sequenced on a sequencing platform (Illumina HiSeq Xten, Illumina, CA, USA) at Guangdong Magigene Biotechnology Co., Ltd. (Guangzhou, China). Raw data quality was trimmed and quality controlled using Trimmomatic v0.36 (Bolger et al., 2014) and the rRNA sequences were removed using Bowtie2 v2.33 (Langmead and Salzberg, 2012). The read counts and functional information of each gene were obtained using HTSeq-count v0.9.1 (Anders et al., 2015), after mapping the remaining mRNA sequences to the reference zebrafish genome using HISAT2 v2.1.0 (https://github.com/infphilo/hisat2). The expression level of each gene was determined as RPKM (Eq. S1), and differential expression analysis were carried out using edgeR v3.16.5 (Robinson et al., 2010). KEGG enrichment analysis of differentially expressed genes was implemented using clusterProfiler v3.4.4 (Yu et al., 2012). The more details of liver transcriptome analysis were provided in the Supplementary methods and Table S3.

2.9. Determination of zebrafish swimming behavior

Measurement of impacts of chlorine treatment on adult zebrafish swimming behavior in artificial microcosms does not represent realistic field conditions, so we investigated impacts on swimming in zebrafish larvae to evaluate the neurotoxicity of chlorine on the zebrafish (Jijie et al., 2020; Fraz et al., 2019; Zhao et al., 2021). Zebrafish larvae were cultured in the same conditions as the adult zebrafish in microcosms. At 120 hpf of chlorine treatment, 36 zebrafish larvae were selected for each group and gently placed into 96-well cell culture plates after removal of malformed or dead individuals. We changed the light conditions to evaluate the effects of chlorine on the behavior of zebrafish, which is sensitive to the light. After an initial acclimation period of 20 min, we recorded free swimming distance and time every 60 s under continuous light for 20 min, followed by 2 cycles of 10-min light:10-min dark; swimming behavior was recorded and analyzed using Zebralab Video-Track (ViewPoint Life Sciences, France).

2.10. Statistics and visualization

Diversity (Shannon index) and richness of the aquatic and intestinal microbial communities were calculated at the genus level using the vegan package in R (Dixon, 2003). Principal coordinate analysis (PCoA) and permutational analysis of variance were performed based on Bray-Curtis dissimilarities of microbial community composition (genus level) and the functional potential (KO level) to determine differences between groups using the vegan package, and the results were visualized using the ggplot2 package in R. To determine treatment differences in genera and function, we applied moderated *t*-tests between groups using the limma package in R, as described by Carrión et al. Carrión et al. (2019). Genera and functions that differed were identified when FDR-adjusted *p*-values were < 0.05. Volcano plots of genera were generated using the ggplot2 package in R and functions were plotted using Maptree in the ggraph and tidyverse packages in R. A random forest classification analysis was conducted to detect family level changes in microbial community composition using the randomForest package in R. Interactions between aquatic microbes in the microcosms were estimated using co-occurrence network analysis, based on the 292 genera with a relative abundance $> 0.01\%$ in at least one sample. We analyzed the correlations between the genera using pairwise Spearman's rank correlations (r) in the psych package in R. We used strong ($r > 0.8$ or $r < -0.8$) and significant ($p < 0.05$) correlations in the network analysis, using Gephi v0.9.2. Modular analysis and average clustering coefficient calculations were run in Gephi v0.9.2, while normalized degree and betweenness centrality (providing information on how critical an OTU in the network) of each node were determined using the igraph package in R. Bubble plots of normalized degree and betweenness centrality were visualized using the ggplot2 package in R. Boxplots, histograms, and scatter plots were visualized using GraphPad Prism v7.00, heatmaps were constructed using the pheatmap package in R, and Venn diagram analysis was performed using the online website "jvenn" (Bardou et al., 2014). Two-tailed Welch's *t*-test was performed to analyze the significant differences between the control and treatments in Analysis Tools of Excel (Microsoft Corporation, Redmond, WA, USA).

3. Results

3.1. Degradation of active chlorine and dynamic changes in microcosm physicochemical properties

We determined degradation rates of active chlorine in pond water treated with different concentrations of sodium hypochlorite and found that rates were more rapid at lower chlorine concentrations, where full degradation occurred within 30 min of treatment with 1.0 and 2.0 mg/L of active chlorine (Fig. S1). Based on this result, we speculated that active chlorine with the initial concentrations of 0.01 and 0.1 mg/L was degraded more quickly within 30 min, although we could not accurately plot the degradation curve by amplifying the chlorine dose. Content of the TDN and TDP of pond water + zebrafish microcosms maintained at 0, 0.01, and 0.1 mg/L of active chlorine did not change over the 14-d experimental period, while levels of pH significantly decreased under chlorine treatment ($p < 0.05$; Fig. S2).

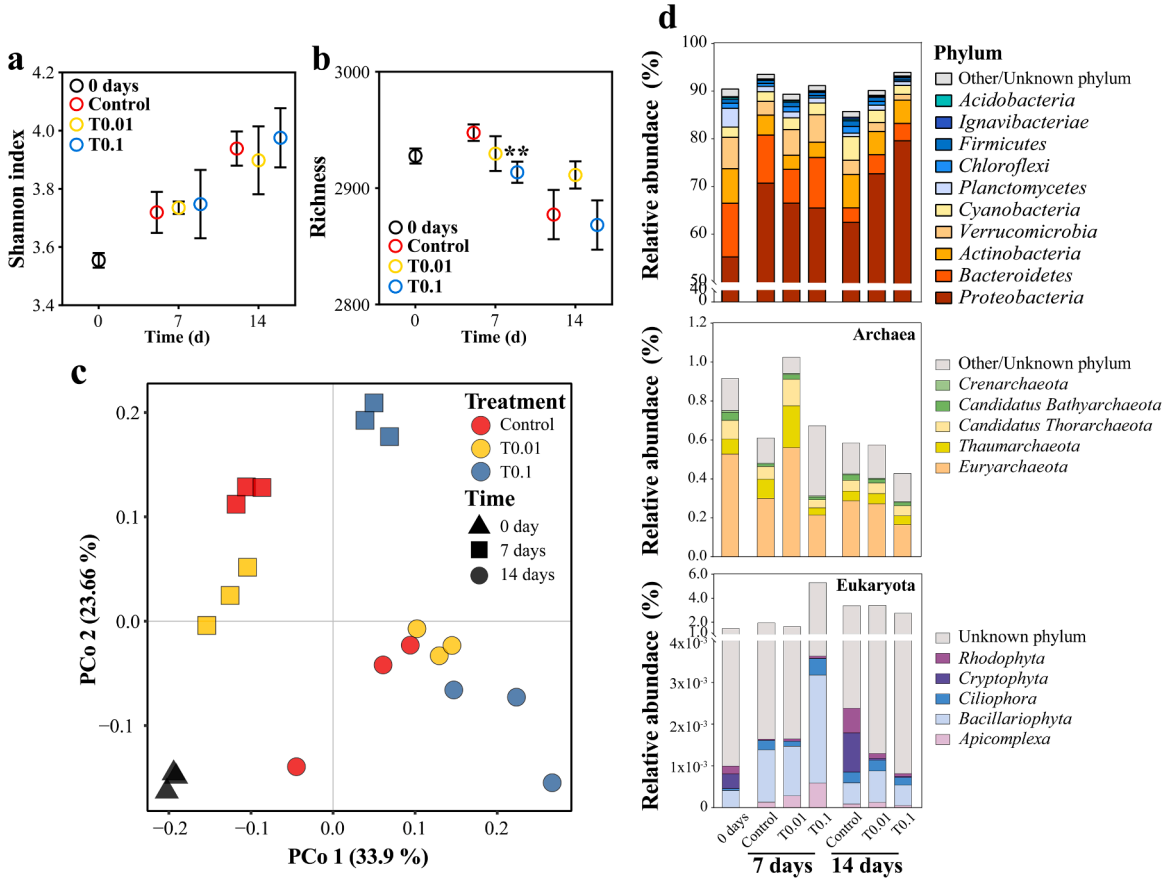

Fig. 1. Effects of chlorine on diversity and structure of microbial communities. Microbial communities at 0 d were the same in all microcosms. a, b Shannon index and richness calculated at the genus level. * represents the significant difference between control and chlorine treatments (two tailed Welch's *t*-test, $p < 0.05$). c PCoA of Bray-Curtis dissimilarities of microbial communities at the genus level. d Effects of chlorine on the community composition of the main phyla. Considering that bacteria dominated in all samples, phylum profiles are shown in these three groups respectively for better visualization.

3.2. Effects of chlorine on microbial community diversity and composition

Neither concentration of active chlorine (0.01 and 0.1 mg/L) affected the diversity of the microbial community during the 14-d exposure time (Fig. 1a). Species richness was lower in microcosms treated with 0.1 mg/L of active chlorine than the control after 7 d of exposure (two-tailed Welch's *t*-test, $p = 0.007$) but recovered after 14 d (Fig. 1b). Although there was little impact of chlorine treatment on microbial community diversity and richness, PCoA with Bray-Curtis dissimilarity showed that both concentrations of chlorine significantly changed the community composition at 7 ($p = 0.006$) and 14 d ($p = 0.004$; Fig. 1c and Fig. S3).

Compared with the control, 676 and 755 genera were significantly affected under the 0.1 mg/L of chlorine treatment after 7 and 14 d, respectively. And 286 and 306 genera were significantly affected under the 0.01 mg/L of chlorine treatment after 7 and 14 d, respectively (Fig. S4). The abundance of the bacteria significantly decreased after 7 d, but increased after 14 d under chlorine treatment, compared to the control (Figs. S5, S6). Analysis of effects of chlorine on abundance of bacteria phyla showed decrease in *Proteobacteria* and increase in *Verrucomicrobia*, *Chloroflexi*, and *Firmicutes* after 7 d in the 0.01 mg/L chlorine treatment, with opposite effects on these phyla recorded after 14 d (Fig. 1d and Fig. S7). A random forest machine learning algorithm, which was used to detect changes in microbial community composition at the family level, selected 43 families with a mean decrease accuracy of > 2.0 as the most sensitive to chlorine. Most of these families belonged to the *Proteobacteria* (n = 20), *Actinobacteria* (n = 7), and *Firmicutes* (n = 5) and were present a low relative abundance (relative abundance of only 10 families was >0.1%) (Fig. S8). Specifically, chlorine treatment promoted the growth of bacteria belonging to families that contains the pathogenic genus, such as the *Mycobacteriaceae*.

The eukaryotes and archaea were recorded at much lower levels of relative abundance than bacteria. Other than increases in abundance of eukaryotes in the 0.1 mg/L of chlorine treatment after 7 d, there were no

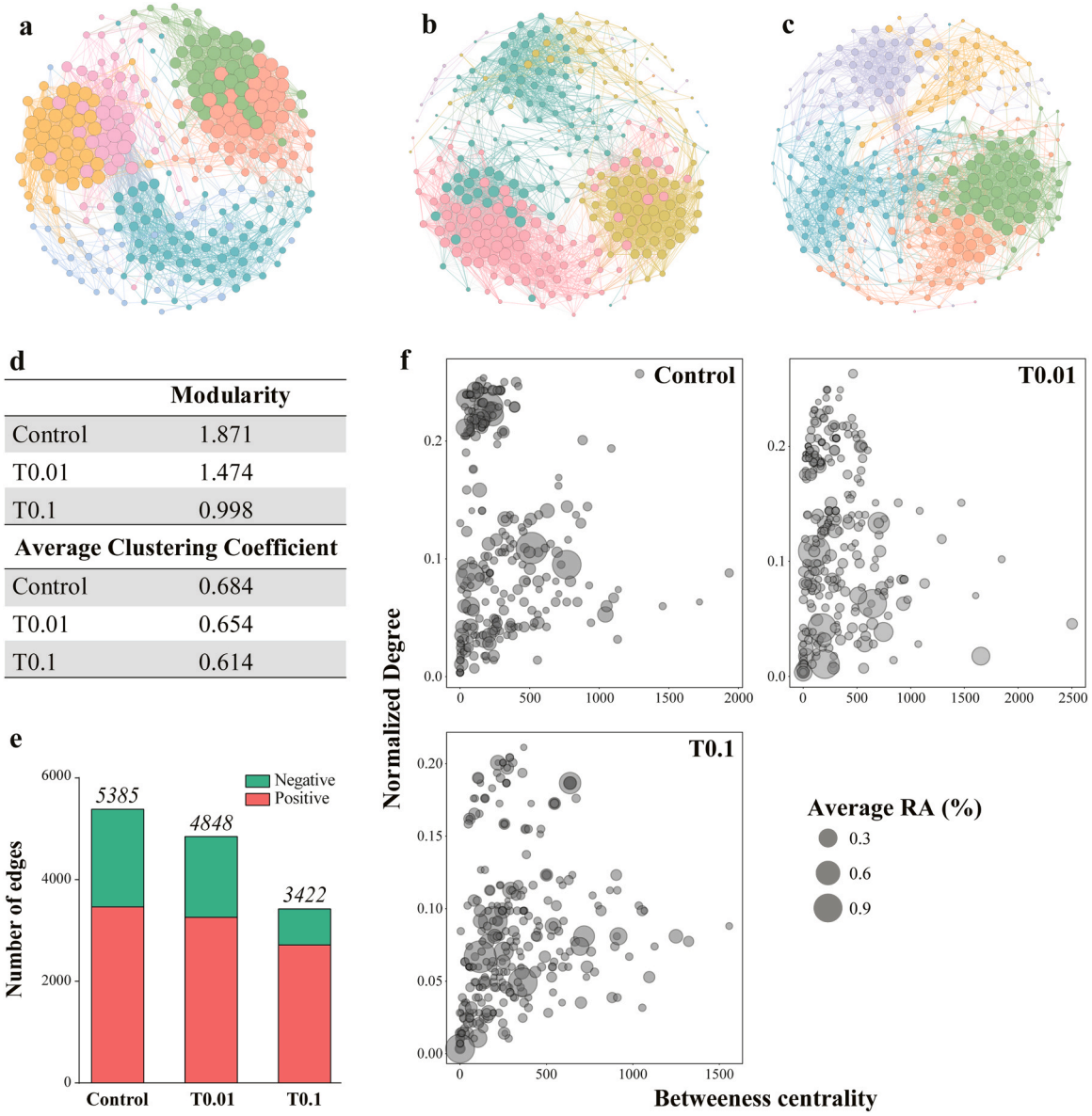

Fig. 2. Effects of chlorine on microbe genus co-occurrence networks. a-c Co-occurrence patterns of genera in the control (a) and 0.01 (b) and 0.1 (c) mg/L of chlorine treatments. Nodes are colored according to module for clearer visualization, and node size represents the number of connections. d Modularity and average clustering coefficients of co-occurrence networks. e Number of negative and positive edges in the microbe co-occurrence networks. Values in italics indicate total number of connections. f Connectedness (normalized degree) and centrality (betweenness centrality) properties of network nodes. The size of nodes represents the average relative abundance (RA) in all samples.

clear consistent effects of chlorine treatment on their abundance (Fig. S5). The *Euryarchaeota* dominated the Archaea, with increases in the 0.01 mg/L of chlorine treatment after 7 d and decreases under the two levels of chlorine concentration after 14 d. Changes in other abundant Archaea phyla were similar to those of the *Euryarchaeota* (Fig. 1d and Fig. S9). Eukaryota was the second most abundant domain but most of its phyla were unidentified. Chlorine treatment affected the abundance of all Eukaryotal phyla (Fig. 1d).

Co-occurrence networks, which based on Spearman's rank correlation coefficients between genera, showed marked differences for microcosms with or without chlorine treatments (Fig. 2a–c). There were decreases in modularity and average clustering coefficient indexes of microbial communities under chlorine treatment, compared to the control (Fig. 2d). The number of interactions of aquatic microbes decreased with increasing chlorine concentration, particularly the negative interactions (Fig. 2e). With increasing chlorine concentration, the number of genera with high levels of connectedness (which defined as the normalized degree in this study) and low levels of betweenness centrality decreased, where abundance of most of these genera was low (Fig. 2f).

3.3. Effects of chlorine on microbial community function potential

As we expected, microbial community function potential was perturbed by chlorine treatment (Fig. 3 and Fig. S10), due to the shift in taxonomic composition (Fig. S3). Almost every function pathway was affected after 7 d of treatment with 0.1 mg/L of chlorine (FDR-adjusted $p < 0.05$), albeit with low degree ($|\log2(\text{fold change})| < 1$) (Fig. 3a and Fig. S11). Unlike the changes in microbial community composition (increases in the number of significantly different genera with time), most regulated pathways had recovered after 14 d (Fig. 3b).

To understand these effects of 0.1 mg/L of chlorine on the function potential in greater detail, we analyzed pathways that were significantly (FDR-adjusted $p < 0.05$) and sharply ($|\log2(\text{fold change})| > 1$) affected (Fig. S12). After 7 d, most functions associated with metabolism, such as flavone and flavonol biosynthesis, geraniol degradation, and xenobiotic biodegradation and metabolism, had decreased, whereas functions associated with environmental information processing, cellular processes, and genetic information processing had been enriched by chlorine. In contrast, most functions associated with metabolism had become enriched by chlorine after 14 d, whereas nine functions associated with environmental information processing decreased (Fig. S12). By this time, some cellular processes, such as biofilm formation-*Pseudomonas aeruginosa* (ko02025), had also become enriched by chlorine treatment (Fig. S12).

3.4. Chlorine impacts on opportunistic human pathogens and ARGs

Continuous inputs of chlorine elicited changes in the structure of the microbial community, including the prevalence of opportunistic human pathogens that are injurious to human health. Seventy-three human pathogen species were detected both in the control and chlorine-treated microcosms (Fig. S13). Annotation of taxonomic information of ARGs also detected five potential antibiotic-resistant pathogens (ARPs) (*Streptococcus pneumoniae*, *Enterobacter cloacae*, *Acinetobacter baumannii*, *Escherichia coli*, *Pseudomonas aeruginosa*). While most pathogens and some ARPs were inhibited after 14 d (Fig. 4a–c), a part of pathogens remained present at high levels of abundance, such as *P. aeruginosa* and species belonging to the *Mycobacteriaceae* (*Mycobacterium leprae*, *Mycobacterium chimaera*, and *Mycobacterium tuberculosis*) (Fig. 4a).

In total, 805 ARGs were detected from the control and chlorine microcosms, and we found that chlorine affected their transfer and prevalence. Horizontal gene transfer (HGT) and vertical gene transfer (VGT) potentials of ARGs were further determined: 560 ARGs were carried by plasmid, whereas only 232 ARGs were carried on the chromosome. Besides, 145 ARGs were carried by both plasmid and chromosome and 158 ARGs could not be clearly assigned to either group (Fig. S14). We also determined the composition of ARGs and found that ARGs carried by chromosomes tended to confer multidrug resistance (Fig. 4d), whereas those carried by plasmids tended to confer tetracycline resistance (Fig. 4e). Total abundance of ARGs on chromosomes was linked to abundance of bacteria that had decreased sharply by 7 d of chlorine treatment and subsequently increased by 14 d (Fig. 4d, f). After 7 d, total abundance of ARGs on plasmids decreased following daily addition of 0.01 mg/L of chlorine but was unaffected by 0.1 mg/L of chlorine. After 14 days, total abundance of ARGs on plasmids increased in the two

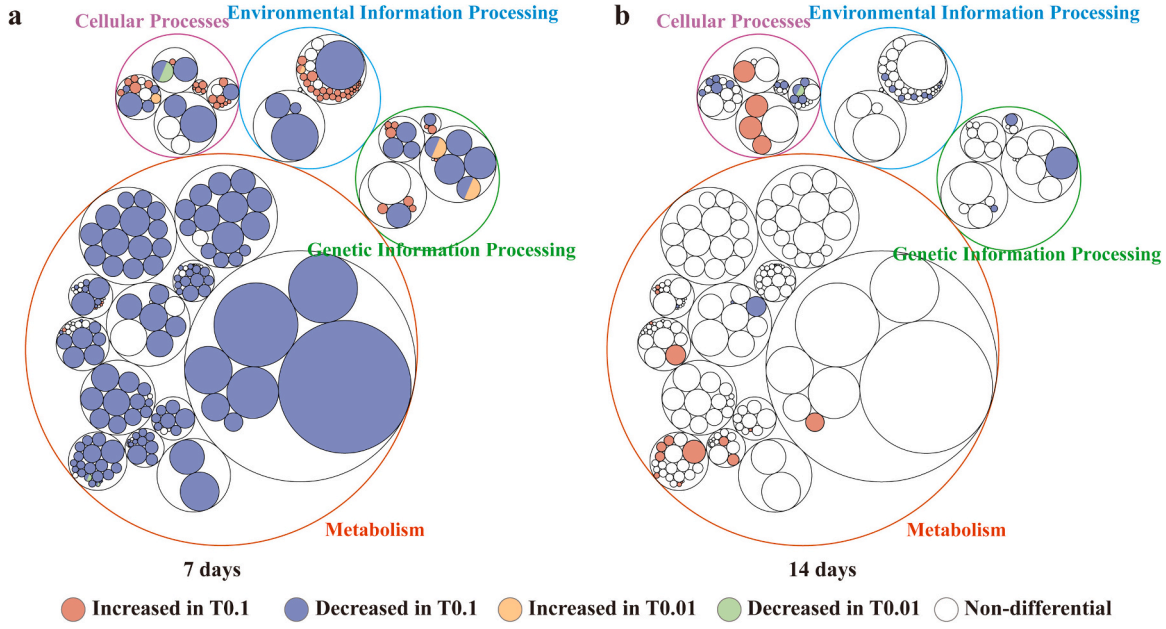

Fig. 3. Effects of chlorine on microbial community functional potential. a Functional potential of microbial community changed under chlorine treatment after 7 d. b Functional potential of microbial community changed under chlorine treatment after 14 d. The outermost circles represent the pathways at the KEGG level 1, while the deepest circles represent pathways at KEGG level 3. Pathways that significantly differed (FDR-adjusted $p < 0.05$) between the control and chlorine treatments are colored as the legends showed. Circle size represents the average relative abundance of pathways in all samples.

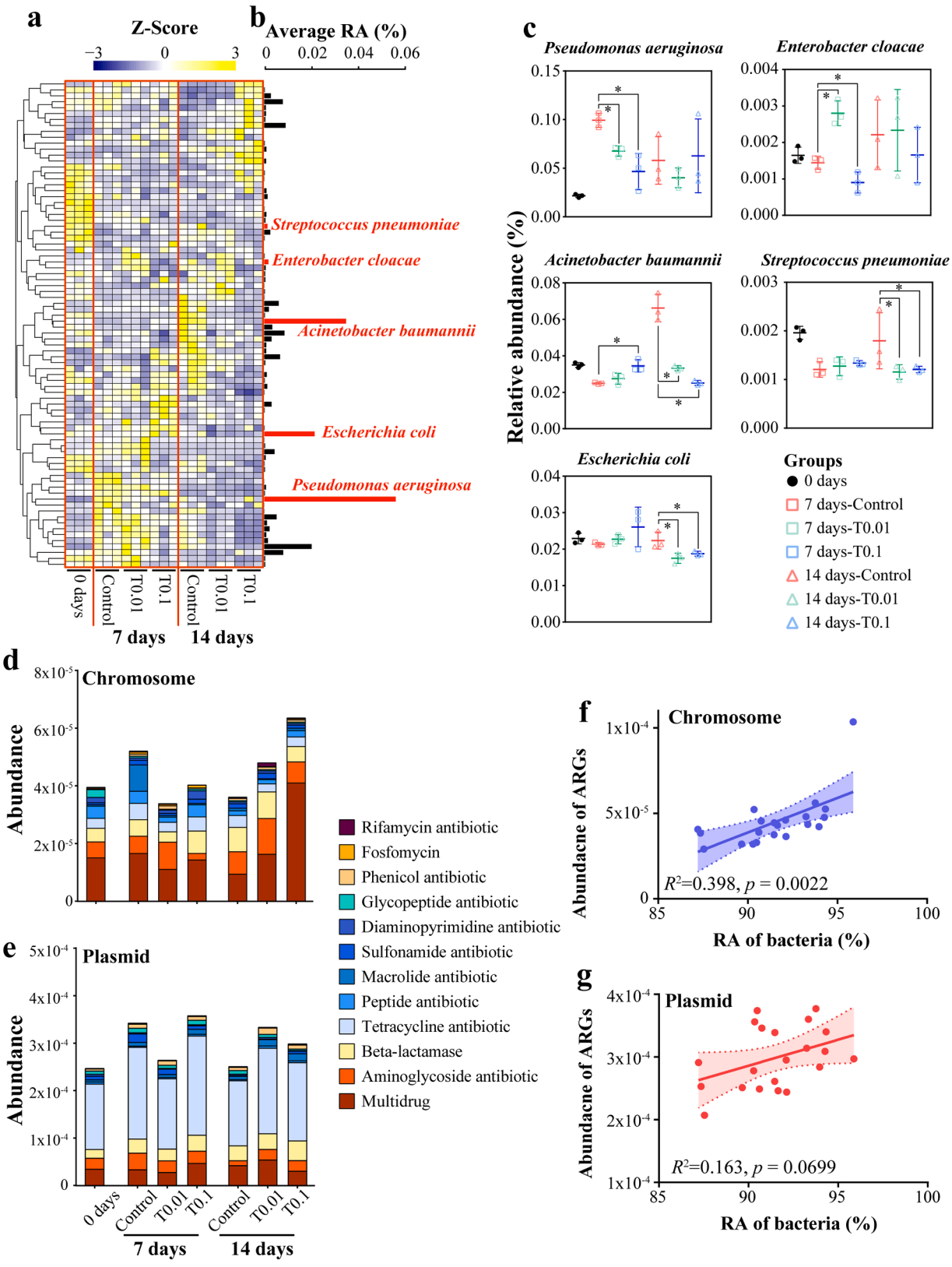

Fig. 4. Effects of chloring on composition of human pathogens and ARGs. a The composition of human pathogens with or without chlorine treatments in 7d and 14d. b Average relative abundance of pathogens in all samples. Antibiotic-resistant pathogens (ARPs) are marked in red. c Relative abundance of ARPs with or without chlorine treatments in 7d and 14d. d and e Compositions of ARGs in chromosomes and plasmids, respectively. Only ARG types detected in all samples are shown. f Linear regression analysis of the relative abundance of bacteria and chromosome-carried ARGs. g Linear regression analysis of the relative abundance of bacteria and plasmid-carried ARGs. Dotted line shows 95% confidence interval. RA: Relative abundance; * represents the significant difference between the control and chlorine treatments (two tailed Welch's *t*-test, $p < 0.05$).

chlorine treatments (Fig. 4e). Unlike the ARGs carried by chromosomes, abundance of plasmid-carried ARGs was not linked to the relative abundance of bacteria (Fig. 4g).

3.5. Chlorine-mediated changes in zebrafish intestinal microbial communities

The diversity and structure of zebrafish intestinal microbial communities with or without chlorine treatment were determined using 16S rRNA gene sequencing. Microbial community richness and diversity (Shannon index) decreased after 7 d of treatment with 0.1 mg/L of chlorine and then recovered by 14 d, and there were no effects of 0.01 mg/L of chlorine. PCoA with Bray-Curtis dissimilarity also showed that intestinal microbial communities changed significantly in 7d but recovered in 14d under chlorine treatment, compared to the control (Fig. 5a–c; Table S4). Chlorine affected the composition of the majority of genera by 7 d of treatment. However, these effects had been reverted by 14 d (Fig. 5d). The transcriptome of zebrafish livers was analyzed to quantify changes in host status following dysbiosis of the intestinal microbial community by 0.1 mg/L of chlorine after 7 d. We found that genes regulated by chlorine tended to be related to the endocrine system and fundamental metabolism of zebrafish (Fig. 5e). We also assessed effects of chlorine on zebrafish larvae swimming behavior to and found that swim speeds were reduced (Fig. 5f).

4. Discussion

While the utility of chlorine-containing disinfectant in disease

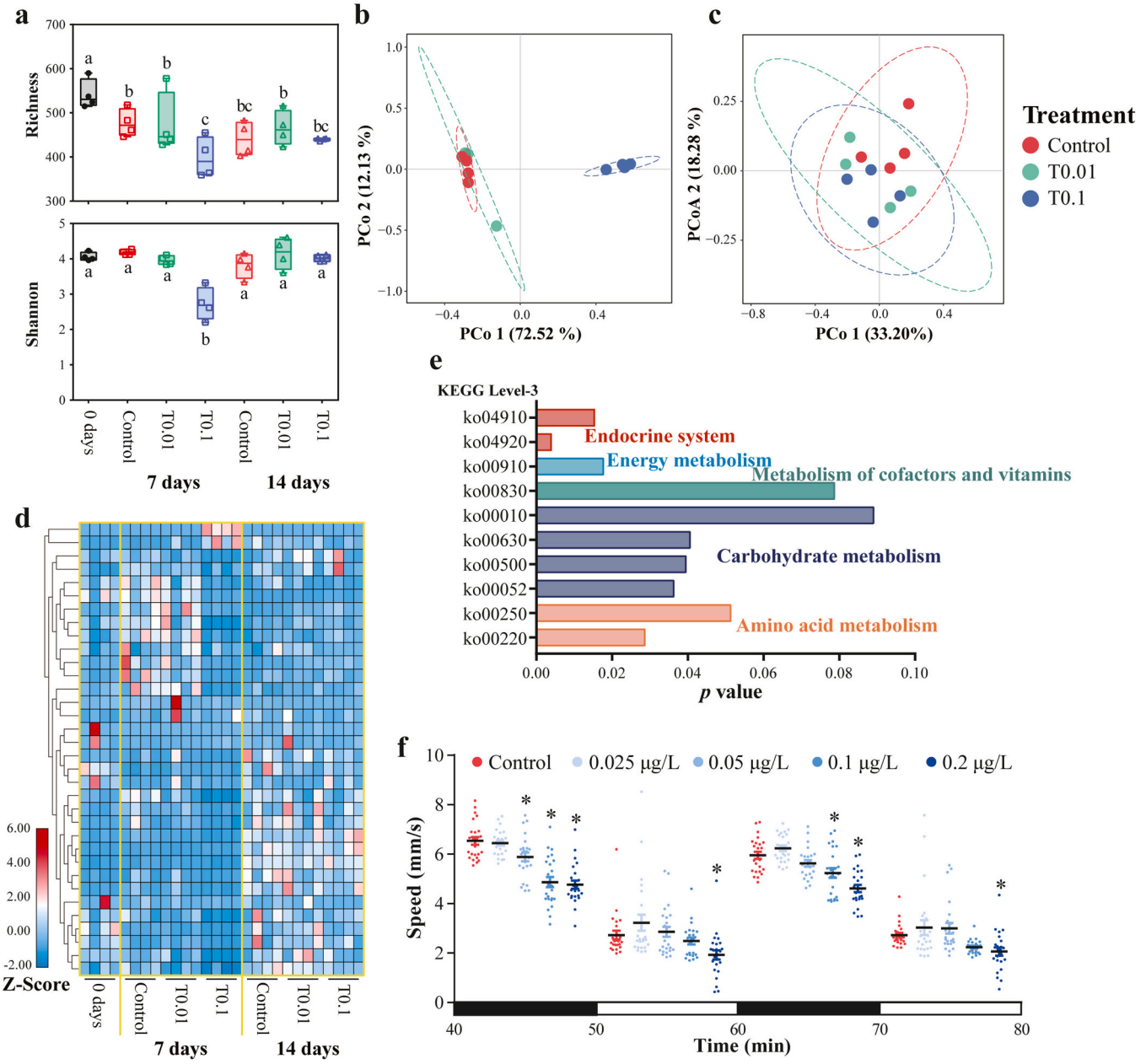

Fig. 5. Effects of chlorine on zebrafish intestinal microbial communities. a Richness (upper panel) and Shannon index (below panel) of the intestinal microbial community at the genus level in each group. b and c PCoA of Bray-Curtis dissimilarity of intestinal microbial community at the genus level at 7 and 14 d, respectively. Ellipse shows 95% confidence interval. d Composition of core genera with or without chlorine treatments. e KEGG level-3 pathways changed in zebrafish liver after treatment for 7 d with 0.1 mg/L of chlorine. Color of pathway represents the KEGG level 2. f Effects of chlorine with different concentrations on zebrafish larvae swimming speed. * represents the significant difference between the control and chlorine treatments (two tailed Welch's *t*-test, $p < 0.05$).

control and water safety is widely accepted (World Health Organization, 2020b), it is essential that the associated environmental risks to freshwater ecosystems are adequately evaluated. In this study, we developed a freshwater microcosm and demonstrated impacts of continuous chlorine treatment on microbial communities and antibiotic resistomes using shotgun metagenome and 16S rRNA gene sequencing.

Although chlorine is rapidly degraded quickly in freshwater, active chlorine disrupted the structure and function of the microbial community. In this study, we found that microbe diversity and richness were not reduced by chlorine at concentrations less than those suggested by WHO (World Health Organization, 2020b) for the effective disinfection of drinking water distribution systems. Under environmental perturbation, microbial community diversity and function may be maintained by shifts in community structure and effects of redundancy (Allison and Martiny, 2008; De Vrieze et al., 2017; Louca et al., 2018). Similarly, our results showed that even though microbial community composition shifted under continuous chlorine treatment, diversity was maintained throughout the experiment and the basic metabolic potential was recovered after 14 d.

Rather than inhibition of bacteria, continuous treatment with a low concentration of chlorine increased bacteria abundance after 14 d. Similar to soils (Qian et al., 2020), freshwater acts as a pool for human pathogens and the increase in bacteria reported here may represent a negative effect of chlorine inputs on freshwater ecosystems and human health. For example, after 14 d of continual treatment with chlorine, there was an increase in abundance of the pathogens *M. leprae*, *M. chimaera,* and *M. tuberculosis* that are closely related to human diseases (De Benedictis et al., 2020; Furin et al., 2019; Steinmann et al., 2017). Some species of bacteria are known to be highly resistant to chlorination and their abundance has been shown to increase under treatment with chlorine-containing disinfectants (Pinel et al., 2020; Macauley et al., 2006). Residual chlorine kills bacteria or inhibits their growth, principally through the overproduction of reactive oxygen species (ROS) (Guo et al., 2015). However, this process may also protect some bacteria and even promote growth of them, depending on levels of ROS (Van Acker and Coenye, 2017; Nguyen et al., 2011; Shatalin et al., 2011). Our results indicate that continuous low concentrations of chlorine may induce subinhibitory concentrations of ROS in most chlorine-resistant bacteria and promote cell growth, rather than mortality. Increased bacterial biomass under chlorination may also be a result of biofilm formation that provides bacteria with nutrients and offers protection against disinfectants (Paranjape et al., 2020). Although we recorded no evidence of the formation of biofilm in the microcosms, abundance of the biofilm forming-*Pseudomonas aeruginosa* was enriched, along with the recovery in growth of *P. aeruginosa*, after 14 d of daily treatment with 0.1 mg/L of chlorine treatment.

Interactions among microorganisms are complex and can be determined by co-occurrence networks (De Vries et al., 2018; Faust and Raes, 2012; Liu et al., 2020). These interactions play a critical role in microbial community assembly, as dominant drivers of population structure and dynamics (Cordero and Datta, 2016; Hansen et al., 2007). The changes in microbial community composition, as a result of chlorine treatment, also disrupted interactions among microorganisms. Although the co-occurrence networks showed the modular structure of the microbial community was maintained, its modularity, average clustering coefficient, and number of interactions decreased. The chlorine-mediated decrease in complexity, defined as the total number of both negative and positive interactions of aquatic microbes, of the freshwater microbial community possibly disrupted its assembly and dynamic changes. This result may be related to increases in selective pressures (Dai et al., 2020). It has been reported that interactions buffer against disturbance (Konopka et al., 2015; Ziegler et al., 2018) and the presence of negative interactions increases the stability of perturbed communities (Coyte et al., 2015; Stouffer and Bascompte, 2011). The loss of interactions among microorganisms in chlorine-treated microcosms, particularly the negative one, may decrease microbial community stability. Keystone taxa are characterized by high levels of connectedness and low levels of betweenness-centrality that support community stability (Berry and Widder, 2014; Xue et al., 2018). The decline in potential keystone taxa by chlorine treatment in our study may also cause lower stability. While the machine learning analysis based on the random forest showed families with low levels of abundance were sensitive to chlorine treatment, we also found that the majority of potential keystone taxa in the chlorine treatments were low-abundance taxa, indicating that rare taxa may play an important role in maintaining the stability of microbial communities under chlorine treatment.

As discussed above, the metabolic potential of the microbial community exposed to chlorine recovered after 14 d, due to functional redundancy (Louca et al., 2018). And it is likely that some functional capacities were altered to buffer against impacts of chlorine. After the first week of chlorine treatment, functions of signal transduction and signaling molecules, and their interaction were enriched. Microbe signaling response tends to be induced under biotic and abiotic stress to trigger detoxification processes (Liu et al., 2020; Bickerton et al., 2016; Dufrêne and Persat, 2020), such as an increase in xenobiotic degradation. Therefore, in addition to functional redundancy, microbe signaling response and xenobiotic biodegradation may be alternative strategies for the alleviation of abiotic stress induced under long-term exposure to chlorine.

The risk assessment of impacts of residual chlorine on the abundance and transfer of ARGs and pathogens harmful to human health in freshwater is urgently required (Lu and Guo, 2021). Unlike ultraviolet disinfection, which kills bacteria mainly through DNA deactivation, chlorination inactivates bacteria through oxidative damage (Guo et al., 2015). The subinhibitory concentrations of chlorine and its analogs could induce the SOS response, increase cell permeability, and alter the expression of conjugation-relevant genes that consequently promote the horizontal transfer of ARGs (Mantilla-Calderon et al., 2019; Guo et al., 2015; Jin et al., 2020; Liu et al., 2018; Zhang et al., 2017). ARGs were categorized as chromosome- or plasmid-carried in this study. ARGs located on chromosomes cannot be horizontally transferred between bacteria cells, unless integrated into plasmids (Che et al., 2019). Chromosome-carried ARGs increased abundance directly dependent on the promotion of growth in bacteria when exposed to continuous inputs of chlorine. ARGs located on plasmids are more threatening to human health than those located on chromosomes, because they may be transferred from antibiotic-resistant bacteria (ARB) to non-ARB, along with plasmids (Jin et al., 2020; Che et al., 2019). Our study showed that the abundance of plasmid-carried ARGs increased when exposed to the chlorine treatments and were not strongly correlated with abundance of bacteria. This result confirms that plasmids are a more stable and transferable carrier than bacteria and was difficult to remove by reduced abundances of bacteria. These results reveal that chlorine treatment could promote the ARG dissemination in freshwater habitats by either VGT through bacteria reproduction, or HGT through plasmid transfer between bacteria, where the latter occurred more frequently and represents a greater threat to human health.

In contrast to the aquatic microbial community, that of zebrafish was more conserved and highly resilient to continuous inputs of chlorine. A robust intestinal microbial community is of vital to host health (Duvallet et al., 2017; Sommer et al., 2017). Thus, recovery of intestinal microbial communities from dysbiosis may represent an effective strategy to alleviate toxicity of residual chlorine. Nevertheless, we found that exposure to chlorine negatively impacted the growth of zebrafish through effects on the endocrine system and fundamental metabolism. Besides, chlorine depressed larvae swimming mobility of the zebrafish. The abnormal swimming behaviors, either increased or decreased, could be recognized as the neurotoxicity of pollutants on the zebrafish (Jijie et al., 2020; Fraz et al., 2019; Zhao et al., 2021). These results verified the negative effects of chlorine on the fish in freshwater.

In conclusion, our study concentrated on the effects of continuous inputs of chlorine-containing disinfectants on microbial communities

and ARG dissemination in freshwater habitats, in contrast to previous studies that have tended to focus on effects on wastewater treatment plants, drinking water distribution systems, and other anthropogenic water systems. Our results showed that even low concentration of chlorine with continuous input could disrupt and destabilize the microbial community structure, decrease the metabolic capability of aquatic microbial communities temporarily, promote some potential pathogens growth and accelerate the transfer of ARGs in freshwater. Besides, low concentration of chlorine with continuous input disrupted the intestinal microbial community structure of zebrafish, which resulted in the negative effects of zebrafish growth and behavior. These findings highlight the ecological and human health risks of the widespread use of chlorine-containing disinfectants for disease control.

Ethics approval and consent to participate

This work followed the NIH guide for laboratory animals (NIH Publication No. 85–23, revised 1996) for the care and use of zebrafish.

CRediT authorship contribution statement

Zhenyan Zhang: Data curation, Formal analysis, Visualization, Writing – original draft, Writing – review & editing. **Qi Zhang:** Data curation, Formal analysis, Visualization. **Tao Lu:** Data curation. **Jieyu Zhang:** Data curation. **Liwei Sun:** Conceptualization, Data curation. **Baolan Hu:** Conceptualization. **Jun Hu:** Data curation. **Josep Peñuelas:** Writing – review & editing. **Lizhong Zhu:** Funding acquisition, Supervision, Conceptualization, Writing – review & editing. **Haifeng Qian** Funding acquisition, Supervision, Conceptualization, Writing – review & editing.

Declaration of Competing Interest

The authors declare that they have no known competing financial interests or personal relationships that could have appeared to influence the work reported in this paper.

Data Availability

The original raw sequencing data have been published in the NCBI Sequence Read Archive (SRA) database with the BioProject numbers PRJNA675324 (raw data of metagenome), PRJNA675332 (raw data of intestinal 16S rRNA gene sequencing) and PRJNA675331 (raw data of liver transcriptome of zebrafish). Raw data can also be provided by the corresponding author upon request.

Acknowledgements

This study was financially supported by the consulting research project of Chinese Academy of Engineering (2020-ZD-15), National Natural Science Foundation of China (21777144, 21976161, and 41907210), and Program for Changjiang Scholars and Innovative Research Team in University (IRT_17R97).

Appendix A. Supporting information

Supplementary data associated with this article can be found in the online version at doi:10.1016/j.jhazmat.2021.127152.

References

Allison, S.D., Martiny, J.B.H., 2008. Colloquium paper: resistance, resilience, and redundancy in microbial communities. Proc. Natl. Acad. Sci. USA 105 Suppl 1, 11512–11519.
Anders, S., Pyl, P.T., Huber, W., 2015. HTSeq—a Python framework to work with high-throughput sequencing data. Bioinformatics 31, 166–169.
Bardou, P., Mariette, J., Escudié, F., Djemiel, C., Klopp, C., 2014. jvenn: an interactive Venn diagram viewer. BMC Bioinforma. 15, 293.
Berry, D., Widder, S., 2014. Deciphering microbial interactions and detecting keystone species with co-occurrence networks. Front. Microbiol. 5, 219.
Bickerton, P., Sello, S., Brownlee, C., Pittman, J.K., Wheeler, G.L., 2016. Spatial and temporal specificity of Ca^{2+} signalling in *Chlamydomonas reinhardtii* in response to osmotic stress. N. Phytol. 212, 920–933.
Bolger, A.M., Lohse, M., Usadel, B., 2014. Trimmomatic: a flexible trimmer for Illumina sequence data. Bioinformatics 30, 2114–2120.
Carrión, V.J., Perez-Jaramillo, J., Cordovez, V., Tracanna, V., de Hollander, M., Ruiz-Buck, D., Mendes, L.W., van Ijcken, W.F.J., Gomez-Exposito, R., Elsayed, S.S., Mohanraju, P., Arifah, A., van der Oost, J., Paulson, J.N., Mendes, R., van Wezel, G. P., Medema, M.H., Raaijmakers, J.M., 2019. Pathogen-induced activation of disease-suppressive functions in the endophytic root microbiome. Science 366, 606–612.
Che, Y., Xia, Y., Liu, L., Li, A.-D., Yang, Y., Zhang, T., 2019. Mobile antibiotic resistome in wastewater treatment plants revealed by Nanopore metagenomic sequencing. Microbiome 7, 44.
Chen, Q.L., Cui, H.L., Su, J.Q., Penuelas, J., Zhu, Y.G., 2019. Antibiotic resistomes in plant microbiomes. Trends Plant Sci. 24, 530–541.
Chu, W., Fang, C., Deng, Y., Xu, Z., 2021. Intensified disinfection amid COVID-19 pandemic poses potential risks to water quality and safety. Environ. Sci. Technol. 55, 4084–4086.
Cordero, O.X., Datta, M.S., 2016. Microbial interactions and community assembly at microscales. Curr. Opin. Microbiol 31, 227–234.
Coyte, K.Z., Schluter, J., Foster, K.R., 2015. The ecology of the microbiome: Networks, competition, and stability. Science 350, 663–666.
Dai, Z., Sevillano-Rivera, M.C., Calus, S.T., Bautista-de los Santos, Q.M., Eren, A.M., van der Wielen, P.W.J.J., Ijaz, U.Z., Pinto, A.J., 2020. Disinfection exhibits systematic impacts on the drinking water microbiome. Microbiome 8, 42.
De Benedictis, F.M., Kerem, E., Chang, A.B., Colin, A.A., Zar, H.J., Bush, A., 2020. Complicated pneumonia in children. Lancet 396, 786–798.
De Vries, F.T., Griffiths, R.I., Bailey, M., Craig, H., Girlanda, M., Gweon, H.S., Hallin, S., Kaisermann, A., Keith, A.M., Kretzschmar, M., Lemanceau, P., Lumini, E., Mason, K. E., Oliver, A., Ostle, N., Prosser, J.I., Thion, C., Thomson, B., Bardgett, R.D., 2018. Soil bacterial networks are less stable under drought than fungal networks. Nat. Commun. 9, 3033.
De Vrieze, J., Christiaens, M.E.R., Walraedt, D., Devooght, A., Ijaz, U.Z., Boon, N., 2017. Microbial community redundancy in anaerobic digestion drives process recovery after salinity exposure. Water Res 111, 109–117.
Ding, X., Zhu, J., Zhang, J., Dong, T., Xia, Y., Jiao, J., Wang, X., Zhou, W., 2020. Developmental toxicity of disinfection by-product monohaloacetamides in embryo-larval stage of zebrafish. Ecotoxicol. Environ. Saf. 189, 110037.
Dixon, P., 2003. VEGAN, a package of R functions for community ecology. J. Veg. Sci. 14, 927–930.
Dufrêne, Y.F., Persat, A., 2020. Mechanomicrobiology: how bacteria sense and respond to forces. Nat. Rev. Microbiol 18, 227–240.
Duvallet, C., Gibbons, S.M., Gurry, T., Irizarry, R.A., Alm, E.J., 2017. Meta-analysis of gut microbiome studies identifies disease-specific and shared responses. Nat. Commun. 8, 1784.
Ebenezer, V., Ki, J.-S., 2014. Biocide sodium hypochlorite decreases pigment production and induces oxidative damage in the harmful dinoflagellate *Cochlodinium polykrikoides*. ALGAE 29, 311–319.
Faust, K., Raes, J., 2012. Microbial interactions: from networks to models. Nat. Rev. Microbiol 10, 538–550.
Fraz, S., Lee, A.H., Pollard, S., Srinivasan, K., Vermani, A., David, E., Wilson, J.Y., 2019. Paternal exposure to carbamazepine impacts Zebrafish offspring reproduction over multiple generations. Environ. Sci. Technol. 53, 12734–12743.
Fu, L., Niu, B., Zhu, Z., Wu, S., Li, W., 2012. CD-HIT: accelerated for clustering the next-generation sequencing data. Bioinformatics 28, 3150–3152.
Furin, J., Cox, H., Pai, M., 2019. Tuberculosis. Lancet 393, 1642–1656.
Guo, M.-T., Yuan, Q.-B., Yang, J., 2015. Distinguishing effects of ultraviolet exposure and chlorination on the horizontal transfer of antibiotic resistance genes in municipal wastewater. Environ. Sci. Technol. 49, 5771–5778.
Hansen, S.K., Rainey, P.B., Haagensen, J.A.J., Molin, S., 2007. Evolution of species interactions in a biofilm community. Nature 445, 533–536.
Huson, D.H., Auch, A.F., Qi, J., Schuster, S.C., 2007. MEGAN analysis of metagenomic data. Genome Res 17, 377–386.
Jia, S., Bian, K., Shi, P., Ye, L., Liu, C.-H., 2020. Metagenomic profiling of antibiotic resistance genes and their associations with bacterial community during multiple disinfection regimes in a full-scale drinking water treatment plant. Water Res 176, 115721.
Jijie, R., Solcan, G., Nicoara, M., Micu, D., Strungaru, S.-A., 2020. Antagonistic effects in zebrafish (*Danio rerio*) behavior and oxidative stress induced by toxic metals and deltamethrin acute exposure. Sci. Total Environ. 698, 134299.
Jin, M., Liu, L., Wang, D.-n, Yang, D., Liu, W.-l, Yin, J., Yang, Z.-w, Wang, H.-r, Qiu, Z.-g, Shen, Z.-q, Shi, D.-y, Li, H.-b, Guo, J.-h, Li, J.-w, 2020. Chlorine disinfection promotes the exchange of antibiotic resistance genes across bacterial genera by natural transformation. ISME J. 14, 1847–1856.
Konopka, A., Lindemann, S., Fredrickson, J., 2015. Dynamics in microbial communities: unraveling mechanisms to identify principles. ISME J. 9, 1488–1495.
Krawczyk, P.S., Lipinski, L., Dziembowski, A., 2018. PlasFlow: predicting plasmid sequences in metagenomic data using genome signatures. Nucleic Acids Res. 46, 35 e35-e35.
Langmead, B., Salzberg, S.L., 2012. Fast gapped-read alignment with Bowtie 2. Nat. Methods 9, 357–359.

Li, D., Gu, A.Z., 2019. Antimicrobial resistance: a new threat from disinfection byproducts and disinfection of drinking water? Curr. Opin. Environ. Sci. Health 7, 83–91.
Li, D., Liu, C.-M., Luo, R., Sadakane, K., Lam, T.-W., 2015. MEGAHIT: an ultra-fast single-node solution for large and complex metagenomics assembly via succinct de Bruijn graph. Bioinformatics 31, 1674–1676.
Liu, H., Huang, X., Tan, W., Di, H., Xu, J., Li, Y., 2020. High manure load reduces bacterial diversity and network complexity in a paddy soil under crop rotations. Soil Ecol. Lett. 2, 104–119.
Liu, S.-S., Qu, H.-M., Yang, D., Hu, H., Liu, W.-L., Qiu, Z.-G., Hou, A.-M., Guo, J., Li, J.-W., Shen, Z.-Q., Jin, M., 2018. Chlorine disinfection increases both intracellular and extracellular antibiotic resistance genes in a full-scale wastewater treatment plant. Water Res 136, 131–136.
Louca, S., Polz, M.F., Mazel, F., Albright, M.B.N., Huber, J.A., O'Connor, M.I., Ackermann, M., Hahn, A.S., Srivastava, D.S., Crowe, S.A., Doebeli, M., Parfrey, L.W., 2018. Function and functional redundancy in microbial systems. Nat. Ecol. Evol. 2, 936–943.
Lu, J., Guo, J., 2021. Disinfection spreads antimicrobial resistance. Science 371, 474.
Lu, T., Zhang, Q., Lavoie, M., Zhu, Y., Ye, Y., Yang, J., Paerl, H.W., Qian, H., Zhu, Y.-G., 2019. The fungicide azoxystrobin promotes freshwater cyanobacterial dominance through altering competition. Microbiome 7, 128.
Ma, X., Zhang, Q., Zheng, M., Gao, Y., Yuan, T., Hale, L., Van Nostrand, J.D., Zhou, J., Wan, S., Yang, Y., 2019. Microbial functional traits are sensitive indicators of mild disturbance by lamb grazing. ISME J. 13, 1370–1373.
Macauley, J.J., Qiang, Z., Adams, C.D., Surampalli, R., Mormile, M.R., 2006. Disinfection of swine wastewater using chlorine, ultraviolet light and ozone. Water Res 40, 2017–2026.
Mantilla-Calderon, D., Plewa, M.J., Michoud, G., Fodelianakis, S., Daffonchio, D., Hong, P.-Y., 2019. Water disinfection byproducts increase natural transformation rates of environmental DNA in *Acinetobacter baylyi* ADP1. Environ. Sci. Technol. 53, 6520–6528.
Nguyen, D., Joshi-Datar, A., Lepine, F., Bauerle, E., Olakanmi, O., Beer, K., McKay, G., Siehnel, R., Schafhauser, J., Wang, Y., Britigan, B., Singh, P., 2011. Active starvation responses mediate antibiotic tolerance in biofilms and nutrient-limited bacteria. Science 334, 982–986.
Paranjape, K., Bédard, É., Whyte, L.G., Ronholm, J., Prévost, M., Faucher, S.P., 2020. Presence of *Legionella* spp. in cooling towers: the role of microbial diversity, *Pseudomonas*, and continuous chlorine application. Water Res 169, 115252.
Pinel, I.S.M., Moed, D.H., Vrouwenvelder, J.S., van Loosdrecht, M.C.M., 2020. Bacterial community dynamics and disinfection impact in cooling water systems. Water Res. 172, 115505.
Qian, H., Zhang, Q., Lu, T., Peijnenburg, W.J.G.M., Penuelas, J., Zhu, Y.-G., 2020. Lessons learned from COVID-19 on potentially pathogenic soil microorganisms. Soil Ecol. Lett. 3, 1–5.
Robinson, M.D., McCarthy, D.J., Smyth, G.K., 2010. edgeR: a bioconductor package for differential expression analysis of digital gene expression data. Bioinformatics 26, 139–140.
Rodrigues Macêdo, L.P., Pereira Dornelas, A.S., Vieira, M.M., Santiago de Jesus Ferreira, J., Almeida Sarmento, R., Cavallini, G.S., 2019. Comparative ecotoxicological evaluation of peracetic acid and the active chlorine of calcium hypochlorite: Use of *Dugesia tigrina* as a bioindicator of environmental pollution. Chemosphere 233, 273–281.
Shatalin, K., Shatalina, E., Mironov, A., Nudler, E., 2011. H_2S: a universal defense against antibiotics in bacteria. Science 334, 986–990.
Sommer, F., Anderson, J.M., Bharti, R., Raes, J., Rosenstiel, P., 2017. The resilience of the intestinal microbiota influences health and disease. Nat. Rev. Microbiol 15, 630–638.
Steinmann, P., Reed, S.G., Mirza, F., Hollingsworth, T.D., Richardus, J.H., 2017. Innovative tools and approaches to end the transmission of *Mycobacterium leprae*. Lancet Infect. Dis. 17, e298–e305.
Stouffer, D.B., Bascompte, J., 2011. Compartmentalization increases food-web persistence. Proc. Natl. Acad. Sci. USA 108, 3648–3652.
Truchado, P., Gil, M.I., Suslow, T., Allende, A., 2018. Impact of chlorine dioxide disinfection of irrigation water on the epiphytic bacterial community of baby spinach and underlying soil. PLoS One 13, 0199291.
Van Acker, H., Coenye, T., 2017. The role of reactive oxygen species in antibiotic-mediated killing of bacteria. Trends Microbiol 25, 456–466.
Vannoni, M., Creach, V., Barry, J., Sheahan, D., 2018. Chlorine toxicity to *Navicula pelliculosa* and *Achnanthes* spp. in a flow-through system: the use of immobilised microalgae and variable chlorophyll fluorescence. Aquat. Toxicol. 202, 80–89.
Wang, J., Shen, J., Ye, D., Yan, X., Zhang, Y., Yang, W., Li, X., Wang, J., Zhang, L., Pan, L., 2020a. Disinfection technology of hospital wastes and wastewater: Suggestions for disinfection strategy during coronavirus disease 2019 (COVID-19) pandemic in China. Environ. Pollut. 262, 114665.
Wang, J., Zhang, B., Duan, H., Liang, C., Sun, H., Zhang, J., Shen, J., Zhang, L., 2020b. Key points of the program for disinfection technology in special places during the coronavirus disease-2019 (COVID-19) outbreak. China CDC Wkly. 2, 140–142.
World Health Organization. 2020a. WHO coronavirus disease (COVID-19) dashboard. https://www.biomedcentral.com/getpublished/writing-resources/references.
World Health Organization. 2020b. Water, sanitation, hygiene, and waste management for SARS-CoV-2, the virus that causes COVID-19. https://www.who.int/publications/i/item/water-sanitation-hygiene-and-waste-management-for-covid-19.
Xue, Y., Chen, H., Yang, J.R., Liu, M., Huang, B., Yang, J., 2018. Distinct patterns and processes of abundant and rare eukaryotic plankton communities following a reservoir cyanobacterial bloom. ISME J. 12, 2263–2277.
Yu, G., Wang, L.-G., Han, Y., He, Q.-Y., 2012. clusterProfiler: an R package for comparing biological themes among gene clusters. OMICS 16, 284–287.
Zhang, Q., Zhang, Z., Lu, T., Peijnenburg, P.W.J.G.M., Gillings, M., Yang, X., Chen, J., Penuelas, J., Zhu, Y.-G., Zhou, N.-Y., Su, J.-Q., Qian, H., 2020. Cyanobacterial blooms contribute to the diversity of antibiotic-resistance genes in aquatic ecosystems. Commun. Biol. 3, 737.
Zhang, Y., Gu, A.Z., He, M., Li, D., Chen, J., 2017. Subinhibitory concentrations of disinfectants promote the horizontal transfer of multidrug resistance genes within and across genera. Environ. Sci. Technol. 51, 570–580.
Zhang, Z., Fan, X., Peijnenburg, W.J.G.M., Zhang, M., Sun, L., Zhai, Y., Yu, Q., Wu, J., Lu, T., Qian, H., 2021. Alteration of dominant cyanobacteria in different bloom periods caused by abiotic factors and species interactions. J. Environ. Sci. 99, 1–9.
Zhao, Y., Liang, J., Meng, H., Yin, Y., Zhen, H., Zheng, X., Shi, H., Wu, X., Zu, Y., Wang, B., Fan, L., Zhang, K., 2021. Rare earth elements lanthanum and praseodymium adversely affect neural and cardiovascular development in Zebrafish (*Danio rerio*). Environ. Sci. Technol. 55, 1155–1166.
Zhu, W., Lomsadze, A., Borodovsky, M., 2010. *Ab initio* gene identification in metagenomic sequences. Nucleic Acids Res 38, 132 e132-e132.
Ziegler, M., Eguíluz, V.M., Duarte, C.M., Voolstra, C.R., 2018. Rare symbionts may contribute to the resilience of coral–algal assemblages. ISME J. 12, 161–172.